Research article

JGS
Journal of the Geological Society

https://doi.org/10.1144/jgs2025-210 | Vol. 183 | 2026 | jgs2025-210

A metasedimentary outlier of the Laurentian continental margin preserved on the Tonian Loch Ness Supergroup, Scottish Caledonides

R. A. Strachan[1]*, A. R. Prave[2,3], A. Morton[4,5], D. Frei[6], K. Kirsimäe[3] and K. A. Cutts[7]

[1] Institute of the Earth and Environment, University of Portsmouth, Burnaby Road, Portsmouth PO1 3QL, UK
[2] School of Earth and Environmental Sciences, University of St Andrews, Bute Building, Queen's Terrace, St Andrews KY16 9TS, UK
[3] Department of Geology, University of Tartu, Ravila 14A, 50411 Tartu, Estonia
[4] Department of Geology and Geophysics, University of Aberdeen, Meston Building, King's College, Aberdeen AB24 3UE, UK
[5] CASP, West Building, Madingley Rise, Madingley Road, Cambridge CB3 0UD, UK
[6] Department of Earth Sciences, University of Western Cape, Robert Sobukwe Road, Bellville, Cape Town, South Africa
[7] Geological Survey of Finland, PO Box 96, FI-02151 Espoo, Finland

RAS, 0000-0002-9568-0832; ARP, 0000-0002-4614-3774; AM, 0000-0001-5649-4183; DF, 0000-0002-3734-737X; KK, 0000-0002-1221-3623; KAC, 0000-0002-7190-1944

*Correspondence: rob.strachan@port.ac.uk

Abstract: The identification of orogenic unconformities in the high-grade internal zones of orogens requires a multidisciplinary approach. In the northern Scottish Caledonides, isolated occurrences of marble and schist (some kyanite-bearing) do not appear to be integral to the Tonian Loch Ness Supergroup and their affinities are controversial. At Glen Urquhart, structural evidence rules out an allochthonous setting for a kyanite schist–marble succession. Petrological evidence indicates contrasting peak metamorphic conditions between kyanite schist (7–8 kbar and 650°C) and adjacent Tonian paragneiss (9 kbar and 700°C). The U–Pb ages obtained from the youngest detrital zircons within a kyanite schist yield a maximum depositional age of *c.* 728 Ma, overlapping the *c.* 725 Ma age of migmatization of the paragneiss. The schist–paragneiss contact is thus interpreted as a tectonically modified unconformity. C–O isotope data from associated marbles and other marble occurrences across the Loch Ness Supergroup suggest correlation with marbles of the late-Cryogenian Easdale Subgroup (Dalradian Supergroup) east of the Great Glen Fault. Deposition of lower parts of the Dalradian Supergroup is likely to have been restricted to east of the fault, but the basin widened so that younger strata progressively onlapped northwestwards and were deposited unconformably on Tonian migmatitic basement.

Supplementary material: Diagrams and tables that support the geochronological and metamorphic aspects of the paper are available at https://doi.org/10.6084/m9.figshare.c.8213648

Received 25 October 2025; **revised** 11 December 2025; **accepted** 17 December 2025

The recognition of unconformities is often straightforward in forelands and external zones of orogens where angular differences in bedding and contrasts in the intensity of deformation and metamorphism between rock units are likely to be preserved. However, in high-grade internal zones of orogens, unconformities can be eradicated by ductile deformation and metamorphic overprinting, which can lead to a blurring of mineralogical and textural differences between successions of different ages. In such settings, a variety of techniques are needed to demonstrate a basement–cover relationship. Here we present the results of an isotopic and petrological study within the high-grade internal zone of the Scottish Caledonides that provides evidence for: (1) a basement–cover relationship between Tonian–Cryogenian (meta-) sedimentary successions; and (2) a potential link between proximal and distal segments of the Laurentian continental margin.

The internal zone of the Scottish Caledonides occurs between the Moine Thrust and the Highland Boundary Fault, and is transected by the Great Glen Fault (GGF: Fig. 1). The bedrock geology between the Moine Thrust and the GGF forms the Northern Highland Terrane (NHT). The NHT is dominated by thick meta-sandstone (psammite) and meta-siltstone (pelite) successions grouped for many years into the 'Moine Supergroup' (Holdsworth *et al.* 1994). This has recently been reclassified and subdivided into Wester Ross and Loch Ness supergroups (Fig. 1) (Krabbendam *et al.* 2021). The Wester Ross Supergroup includes the unmetamorphosed Torridon Group of the Caledonian foreland and the Morar Group above the Moine Thrust (Fig. 1). It was deposited after *c*. 1000 Ma, the age of the youngest detrital zircons that it contains (Strachan *et al.* 2024 and references therein). The Morar Group was affected by Renlandian (950–930 Ma) amphibolite-facies metamorphism and crustal thickening, which is attributed to the development of an accretionary orogen along the NE Laurentian margin of Rodinia (Cutts *et al.* 2009; Cawood *et al.* 2010; Bird *et al.* 2018; Kinny *et al.* 2025). It is presumed to have then been uplifted and eroded prior to deposition of the younger Glenfinnan and Loch Eil groups of the Loch Ness Supergroup (Fig. 1). The Morar, Glenfinnan and Loch Eil groups were all subsequently affected by multiple tectonothermal events (820–780 and 740–725 Ma) that are referred to collectively as Knoydartian and which are also thought to result from accretionary orogenesis (Cawood *et al.* 2010, 2015; Cutts *et al.* 2010; Kinny *et al.* 2025). South of the GGF, an inlier of the Loch Ness Supergroup (Badenoch Group) is overlain by the Dalradian Supergroup (Fig. 1).

Dalradian deposition was initiated during the Tonian in a Knoydartian foreland basin, whereas its Cryogenian–early Ordovician phase records rifting and break-up of Rodinia and

© 2026 The Author(s). This is an Open Access article distributed under the terms of the Creative Commons Attribution License (http://creativecommons.org/licenses/by/4.0/). Published by The Geological Society of London. Publishing disclaimer: https://www.lyellcollection.org/publishing-hub/publishing-ethics

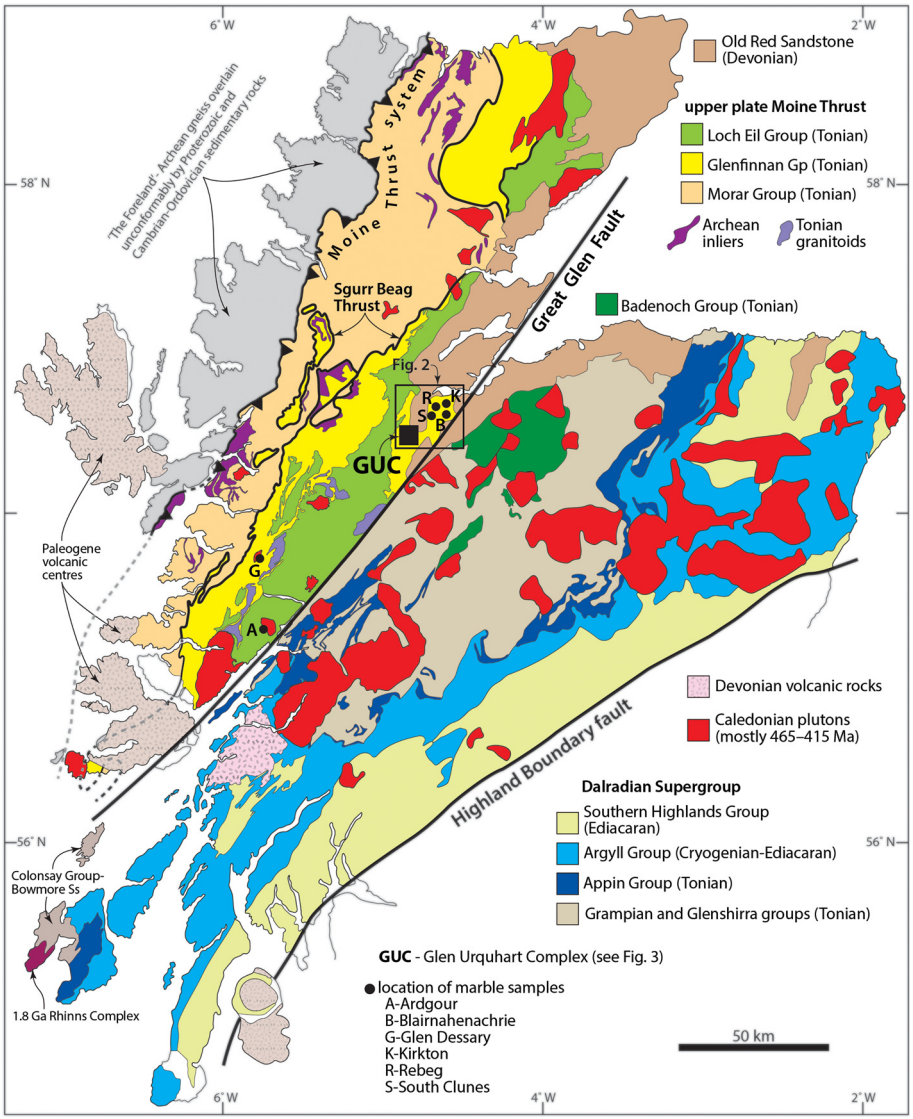

Fig. 1. Simplified geology of the Scottish Caledonides and the Hebridean foreland, showing the location of the Glen Urquhart Complex (GUC) and other marble localities within the outcrop of the Glenfinnan and Loch Eil groups (Loch Ness Supergroup).

opening of the Iapetus Ocean (Prave *et al.* 2023, 2024*a* and references therein). The sediments that accumulated during the latter phase were deposited along the distal Laurentian margin, and their proximal, passive-margin counterparts are the shallow-marine Ardvreck and Durness groups of Cambrian–Ordovician age on the Caledonian foreland (Fig. 1). Those rest unconformably on the Archean–Paleoproterozoic Lewisian Gneiss Complex and Stenian–Tonian 'Torridonian' sedimentary rocks (Prave *et al.* 2024*a*). The Caledonian Orogeny occurred in the Ordovician–Silurian and culminated in the collision of Laurentia, Baltica and Avalonia (Law *et al.* 2024; Leslie *et al.* 2024 and references therein).

In the NHT, isolated lenses of interlayered marbles and schists crop out sporadically within the mapped extent of the Loch Ness Supergroup and as xenoliths within Caledonian plutons (Fig. 1). Although Francis (1964) viewed these rocks as an integral part of the adjacent meta-sedimentary bedrock, others have taken an alternative view. On the basis of trace element data, it has been argued that instead they represent a distinctly younger metasedimentary succession, potentially part of a transition between the Cambrian of the foreland and the middle Dalradian (Russell *et al.* 1986), or an entirely separate 'Albynian' succession of unknown and possibly allochthonous origin (Rock *et al.* 1984). The largest and best exposed occurrence is within the 'Glen Urquhart Complex' (Figs 1 and 2), a succession of kyanite schists and marbles, and a serpentinite body (Horne and Hinxman 1914; Francis 1956; Rock *et al.* 1984, 1986; Wicks 1984; Rock and Dabek 1990). Here we use structural and metamorphic analysis, U–Pb zircon geochronology, and C isotopes to reinvestigate the Glen Urquhart Complex with a particular focus on the affinities of the kyanite schist–marble succession. C isotopes are also used to evaluate possible linkages with marble–schist occurrences elsewhere in the Loch Ness Supergroup. We then use these new data to discuss the implications for regional stratigraphic correlations and the ages of tectonic structures.

Geological setting of the Glen Urquhart Complex

Glenfinnan Group

The Glenfinnan Group in the Glen Urquhart area (Fig. 2) comprises psammitic and pelitic paragneiss that are devoid of sedimentary structures (Emery 2005). The dominant gneissic foliation was produced during migmatization that produced metatexites and diatexites. The foliation contains isoclinal intrafolial folds and is likely to be composite. Concordant pods and sheets of garnetiferous amphibolite up to 20 m thick are relatively common and are interpreted as pre-tectonic mafic intrusions. Zircons analysed by Cutts *et al.* (2010) from a sample of migmatite (sample 102/02 in Fig. 2b) were subhedral and elliptical in shape, often comprising zoned cores that were truncated by dark rims that were poorly luminescent under cathodoluminescence and had low Th/U ratios (Cutts *et al.* 2010). The cores were interpreted as original detrital

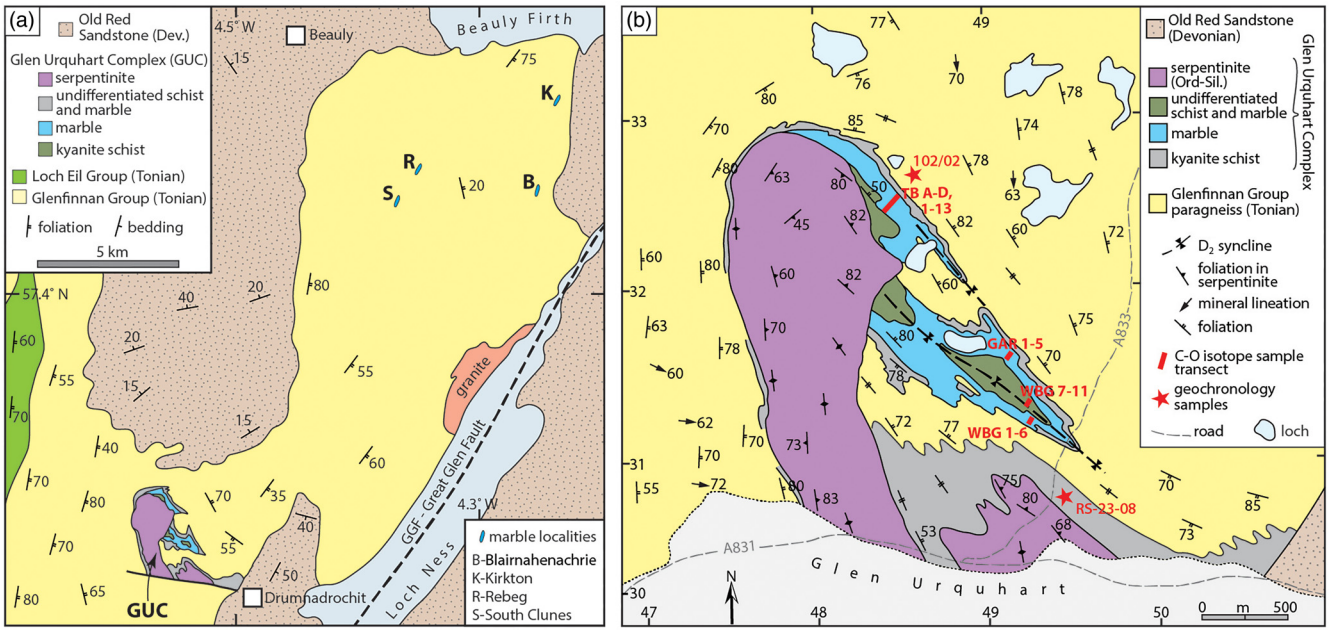

Fig. 2. (**a**) Generalized geology of the area west of Inverness, showing marble occurrences within the Glenfinnan Group. (**b**) Simplified geology of eastern Glen Urquhart. British National Grid numbers are shown along map margins. GAR, Upper Gartully; TB, Torr Buidhe; WBG, Wester Balnagrantacht. 102/02 represents the location of the sample of Glenfinnan Group migmatitic paragneiss analysed by Cutts *et al.* (2010). Source: (a) contains British Geological Survey (2007) materials © UKRI 2007; https://webapps.bgs.ac.uk/data/maps; and (b) modified from Emery (2005) and also contains British Geological Survey materials © UKRI 1990.

grains within the host gneiss and the rims as metamorphic overgrowths formed during migmatization. The cores yielded U–Pb ages mostly in the range of *c.* 1100–1000 Ma, emphasizing the importance of the Grenville orogen in supplying sediment to this area of Laurentia (Cutts *et al.* 2010). The youngest core from a detrital zircon grain was dated at 917 ± 13 Ma, which provides a lower limit for the deposition of the Glenfinnan Group.

Cutts *et al.* (2010) used *in situ* U–Pb geochronology to date monazite inclusions within a zoned garnet from sample 102/02 and documented a complex tectonothermal evolution. Growth of the garnet core occurred at *c.* 825–780 Ma at peak conditions of *c.* 650°C and 7 kbar. This was followed by migmatization at 725 ± 4 Ma, as dated by U–Pb analyses of zircon rims and whole grains with low Th/U ratios contained within a leucosome from the same sample. Monazite inclusions within a second garnet zone yielded an identical age of 724 ± 6 Ma, with metamorphic conditions rising from *c.* 650°C and 6 kbar to *c.* 700°C and 9 kbar. These Neoproterozoic metamorphic events are attributed to Knoydartian orogenesis (Cawood *et al.* 2010, 2015; Cutts *et al.* 2010). Evidence for overprinting by Ordovician (Caledonian) metamorphism is provided by: (1) monazites within the garnet rim that formed at 7 kbar and 650°C at 464 ± 3 Ma (Cutts *et al.* 2010); (2) a U–Pb zircon age of 464 ± 4 Ma obtained from a deformed syntectonic pegmatite (Cutts *et al.* 2010); (3) a Lu–Hf garnet age of 474.8 ± 1.2 Ma from an amphibolite (Bird *et al.* 2013); and (4) a U–Pb monazite age of 473 ± 2 Ma from a paragneiss (Mako *et al.* 2021).

Glen Urquhart Complex

Kyanite schist–marble association

Strips of kyanite schist and marble attain thicknesses of more than 100 m, and are interfolded typically on a scale of tens of metres with each other and the Glenfinnan Group (Fig. 2b) (Francis 1956, 1958; Rock *et al.* 1986; Rock and Dabek 1990). Contacts between these lithologies and Glenfinnan Group paragneisses are relatively sharp with no hint of an original sedimentary transition. The schists are rusty weathering and composed of kyanite–biotite–quartz–plagioclase with accessory graphite, rutile and pyrite. Where affected by retrogression, biotite is replaced by muscovite and/or chlorite. They are not migmatitic and thus contrast sharply with the Glenfinnan Group paragneiss. Locally, they contain metre-scale layers of quartzose psammite. The marbles weather cream- to yellow-grey and occur as bodies many metres to several tens of metres thick. The most common variant is marked by thick, structureless beds and contains diopside–epidote ± tremolite. The most extensively exposed carbonate body is at Torr Buidhe (denoted TB in Fig. 2b and discussed in more detail below), where it is 40–60 m thick and forms a linear ridge several hundreds of metres in length. Contacts between the kyanite schists and the marbles are commonly gradational over a few metres due to the development of Ca–Mg–Fe silicate–carbonate rocks that were interpreted by Francis (1958) and Rock and Dabek (1990) as skarns produced by metasomatism. Concordant pods and sheets of amphibolite occur locally within the kyanite schists and the marbles, but do not carry garnet and are thus distinct from those within the Glenfinnan Group (Rock and Dabek 1990). U–Pb analyses of detrital zircons from a quartzose psammite layer within the kyanite schist yielded age peaks at *c.* 1680–1630, 1510–1490, 1430–1330 and 1100–1040 Ma, identical to those identified within the adjacent Loch Ness Supergroup (Cawood *et al.* 2004).

Serpentinite

The serpentinite forms two main bodies (Fig. 2), which, based on geophysical evidence, are thought to be connected at depth (Rock and Dabek 1990). The western margin of the main body is subvertical and concordant with the country rock Glenfinnan Group. In contrast, the eastern margin of the main body dips eastwards and, although faulted, is strongly discordant on the map scale with the host Glenfinnan Group paragneisses. A smaller body to the east is very poorly exposed. The main lithology is massive to heterogeneously foliated and dominated by a serpentine mesh texture (lizardite and brucite with minor bastite) that encloses relict grains of olivine and enstatite (Francis 1956; Wicks 1984; Rock and

Dabek 1990; Emery 2005). The anastomosing foliation is defined by lenses and stringers of chlorite, magnetite and tremolite. Talc and antigorite occur as late replacements of lizardite and bastite. The igneous parent is thought to have been a harzburgite (Rock and Dabek 1990). Wicks (1984) concluded that the original olivine–pyroxene mineral assemblage underwent initial plastic, solid-state flow, followed by down-temperature deformation, foliation development and pervasive serpentinization during emplacement.

Structural geology and sequence of events

There is evidence for three significant episodes of deformation (D_1–D_3) at Glen Urquhart (Emery 2005; Cutts *et al.* 2010). The dominant folds and associated metamorphic fabrics formed during D_1 and D_2. D_1 formed the high-grade gneissic foliation (S_1) within the Glenfinnan Group that is associated with isoclinal folds and migmatization. D_2 resulted in widespread isoclinal interfolding of the Glenfinnan Group and the kyanite schist–marble association on all scales (Fig. 2b) and transposition of S_1 within the Glenfinnan Group. D_2 axial planes and associated schistosity (S_2) dip moderately east to NE and axes plunge moderately to the SE, parallel to a mineral and stretching lineation. The kyanite schist–marble association appears to occupy the cores of reclined synclinal folds that probably have a large-scale sheath-like geometry. Although there are local 1–10 m-wide zones of intense foliation development close to the contact between the Glenfinnan Group and the kyanite schist–marble association, there is no evidence that they are separated by a large-scale high-strain zone.

Emplacement of the main serpentinite body appears to post-date D_2 folding, as indicated by discordance between these structures and the eastern boundary of the intrusion (Fig. 2b) (Rock *et al.* 1986; Rock and Dabek 1990; Emery 2005). However, in places the internal foliation within the serpentinite is oblique to the eastern boundary of the intrusion yet sub-parallel with the composite S_1/S_2 foliation within the metasediments (Wicks 1984). These field relations are consistent with a late-D_2 age of emplacement for the serpentinite. The large-scale arc defined by the composite S_1/S_2 foliation in the Glenfinnan Group around the northern margin of the intrusion is paralleled by the foliation within the serpentinite. This could be related to progressive emplacement of the intrusion during the late stages of D_2 or, alternatively, due to later D_3 folding. A series of D_3 upright, gentle to open folds that vary from north–south to NW–SE in trend, with gently plunging axes, deform D_1 and D_2 structures and the foliation in the serpentinite. A late-D_2 emplacement age for the serpentinite body means that it is distinctly younger than the host kyanite schist–marble association that was affected by D_2 folding. We do not therefore consider the serpentinite body further.

Other marble occurrences within the Loch Ness Supergroup

Four isolated occurrences of marble, each possibly no more than a few tens to several hundreds of metres in extent, have been documented from small quarries NE of the Glen Urquhart Complex (Figs 1 and 2a) (Horne and Hinxman 1914; Rock *et al.* 1984; Heptinstall 2025). At Rebeg and South Clunes, associated lithologies include calc-schists, pelitic schists, skarns and hornblende–biotite schists. Layers of rather featureless psammite occur interbanded with marble in the Rebeg quarry. Exposures of marble at Blairnahenachrie (no longer accessible) were associated with pelitic gneisses and skarns; and at Kirkton, marble is interbanded with black semi-pelitic schist. Where schistose units are exposed, the main foliation is parallel to lithological layering, and the marbles and associated lithologies at Rebeg, South Clunes and Kirkton are folded, some isoclinally. Contacts with undoubted Glenfinnan Group lithologies are unexposed.

Further SW (Fig. 1), xenoliths of marble occur within the Glen Dessarry Syenite (Harry 1951; Lambert *et al.* 1964; van Breemen *et al.* 1979), which was intruded into the Loch Eil Group at 448 ± 3 Ma (U–Pb zircon: Goodenough *et al.* 2011). Similarly, xenoliths of marble occur at Ardgour within a satellite body of the Glen Scaddle Metagabbro (Drever 1940), which was intruded into the Loch Eil Group at 426 ± 3 Ma (U–Pb zircon: Strachan and Evans 2008). Rock *et al.* (1984) reported that two outcrops of marble here apparently occur *outside* the intrusion within the host Loch Eil Group, but contacts are unexposed.

Sampling rationale and sample characteristics

Given: (a) the lack of any evidence at Glen Urquhart for a significant high-strain zone that would be required if the kyanite schist–marble association was an exotic allochthon; and (b) the textural contrast between the migmatized Glenfinnan Group and the unmigmatized kyanite schists, it is plausible that these are separated by a tectonized unconformity. In order to test this hypothesis we have: (1) assessed the metamorphic conditions of a sample of kyanite schist in order to compare these with the known petrological history of nearby Glenfinnan Group paragneiss (Cutts *et al.* 2010); (2) dated detrital zircons from the same sample in order to establish its maximum depositional age; and (3) sampled marbles for C–O isotopic analyses that might further constrain their depositional age. Monazite and rutile were also analysed from the kyanite schist in order to supplement published data relating to the timing of regional metamorphism. We have also sampled marbles from elsewhere within the Loch Ness Supergroup for C–O isotope analysis for the purpose of comparison with the Glen Urquhart dataset.

Sample RS-23-08: kyanite schist

A kyanite-bearing metapelite in the Glen Urquhart Complex was sampled at NH 4939 3081 (Fig. 2b). It contains kyanite, biotite, plagioclase, quartz, rutile, zircon and muscovite. The rock is compositionally banded on the centimetre scale with alternating quartz–plagioclase-rich and biotite–kyanite-rich bands. Potentially, these reflect originally compositional banding due to deposition with aluminous former mud-rich layers being separated by more sandy quartz–feldspar-rich bands. A strong foliation is defined by biotite and kyanite. Kyanite forms blades up to 5 mm long (more commonly 1–2 mm), and contains inclusions of rutile, zircon and quartz. On grain edges, kyanite is replaced by muscovite. Muscovite also occurs intergrown with matrix biotite. Biotite forms short (up to 1 mm), rounded blades, with larger groups of grains occurring in the biotite–kyanite-rich bands. Rutile occurs as inclusions in kyanite, plagioclase and biotite. Rutile is often rounded but where it is oblong, it is orientated parallel to the matrix foliation. Rutile and zircon are also observed growing together.

Glen Urquhart Complex and other marbles

A total of 97 marble samples was collected for C–O isotope analyses (Supplementary Table 1); collectively, this sample set includes almost all the known occurrences of marbles within the mapped extent of the Loch Ness Supergroup (Figs 1 and 2). Thirty-one samples were collected through the marble units in the Glen Urquhart Complex: 26 are from the commonest occurring marbles, which are thick-bedded, cream-grey weathering and coarsely crystalline, locally with thin pale-green calc-silicate lenses; and five are from a minor variety that is more finely crystalline, weathers yellow-buff and consists of centimetre-thick layers separated by thinner schist intervals and partings. Fifty samples are from the

isolated occurrences of interlayered marble–psammite–pelite units exposed in old quarries NE of the Glen Urquhart Complex (Fig. 2a) and 16 are from xenoliths within the Glen Dessary and Glen Scaddle plutons (Fig. 1). Of these 66 samples, 15 were collected from outcrop and 51 are from the British Geological Survey's archive collection.

Analytical methods

Petrological analysis

Micro-X-ray fluorescence

A rock block from sample RS-23-08 was imaged using a Bruker M4 Tornado Micro-XRF (micro-X-ray fluorescence spectrometer) hosted at the Geological Survey of Finland (GTK) (Supplementary Fig. 1). The system is equipped with a 30 W rhodium (Rh) anode X-ray tube, two 30 mm^2 silicon drift detectors (SDD) with an energy resolution of less than 145 eV (MnKα) at 275 kcps (kilocounts per second) via beryllium windows and polycapillary optics. All data acquisition was performed with an accelerating voltage of 50 kV, a beam current of 500 µA using a fixed spot size of 20 µm under a 2 mbar vacuum. The step size during the analytical run was 40 µm and a pixel dwell time of 20 ms $pixel^{-1}$. The qualitative elemental maps were generated using the Bruker M4 software with later processing in XMapTools (Lanari *et al.* 2014). The map spectra were processed using the Bruker M4 software to produce normalized wt% compositions for the major elements.

Pressure–temperature modelling

Pressure–temperature (*P–T*) pseudosections were calculated for sample RS-23-08 using the software package Theriak–Domino (Capitani and Petrakakis 2010) and the database of Holland and Powell (2011) for the geologically realistic system NCKFMASHTO (Na_2O–CaO–K_2O–FeO–MgO–Al_2O_3–SiO_2–H_2O–TiO_2–Fe_2O_3). The 'metapelite set' of models from White *et al.* (2014*a*), converted to Theriak–Domino format by Doug Tinkham (see Jørgensen *et al.* 2019), were applied. These are White *et al.* (2014*b*) for orthopyroxene, garnet, biotite, staurolite, chloritoid, cordierite and chlorite; White *et al.* (2014*a*) for muscovite and silicate melt; Holland and Powell (2011) for epidote; Holland and Powell (2003) for plagioclase; quartz, H_2O, kyanite, sillimanite and andalusite are also included as pure phases. The absence of garnet from this sample meant that it was not necessary to include MnO in the system. In addition, a lack of Fe^{3+}-bearing phases such as magnetite indicated that including ferric iron in the modelling was unnecessary. A $T - X_{Fe_2O_3}$ diagram was calculated to evaluate the potential effect of higher Fe^{3+} values (Supplementary Fig. 2). This diagram shows that higher contents of Fe^{3+} (greater than 10–15%) produce assemblages containing ilmenite in addition to rutile. For this reason, only 2% iron was set as Fe^{3+} (see the dashed line in Supplementary Fig. 2). A $T - X_{H_2O}$ diagram was calculated to indicate an appropriate H_2O value for the *P–T* diagram (Supplementary Fig. 3). This diagram was contoured for the proportions of muscovite and melt present in the assemblages.

Zircon, monazite and rutile U–Pb geochronology

All U–Pb age data were obtained at the Central Analytical Facility (CAF), Stellenbosch University, by laser ablation-single collector-magnetic sector field-inductively coupled plasma-mass spectrometry (LA-SF-ICP-MS) employing a Thermo Finnigan Element2 mass spectrometer coupled to a Resonetics Resolution excimer laser ablation system equipped with a Laurin Technology S155 two-volume ablation cell.

The zircon age data presented here were obtained by single-spot analyses with a spot diameter of 30 µm and a crater depth of *c.* 15–20 µm. The methods employed for analysis and data processing are described in detail by Gerdes and Zeh (2006), Frei and Gerdes (2009) and Cornell *et al.* (2016). For quality control, the 91500 (Wiedenbeck *et al.* 1995), M127 (Nasdala *et al.* 2008; Mattinson 2010) and Plesovice (Aftalion *et al.* 1989; Sláma *et al.* 2008) zircon reference materials were analysed, and the results were consistently in excellent agreement with the published isotope dilution-thermal ionization mass spectrometry (ID-TIMS) ages. Examination of the internal structures of zircons was carried out by cathodoluminescence (CL) imaging employing a Zeiss Merlin electron microscope at CAF.

For rutile, the age data were obtained by single-spot analyses with a spot diameter of 43 µm and a crater depth of *c.* 15–20 µm. The methods employed for analysis and data processing are similar to those described in detail by Gerdes and Zeh (2006) and Frei and Gerdes (2009). The R10 rutile (Luvizotto *et al.* 2009; Schmitt and Zack 2012) was used as primary calibration material. For quality control, the Thompson Mine (Couëslan *et al.* 2013) and Tabor (Janoušek and Gerdes 2003) rutile reference materials were analysed, and the results were consistently in excellent agreement with the published ages.

Monazite age data were obtained from single-spot analyses with a spot diameter of 9 µm and a crater depth of *c.* 10–15 µm. The methods employed for analysis and data processing are described in detail by Frei and Gerdes (2009) and Cornell *et al.* (2016). The USGS 44069 monazite was used as the primary calibration material (Aleinikoff *et al.* 2006). For quality control, the Thompson Mine (Couëslan *et al.* 2013) and Itambe (Prabhakar 2013) monazite reference materials were analysed, and the results were consistently in excellent agreement with the published ages.

Full analytical details and the results for all quality control materials analysed are reported in Supplementary Tables 2–4. The calculation of concordia ages and plotting of concordia diagrams were performed using Isoplot/Ex 3.0 (Ludwig 2003), and probability–density plots were generated using AgeDisplay (Sircombe 2004). The full analytical dataset is given in Supplementary Table 5.

Carbonate isotopes

Carbonate O and C stable isotope compositions of the samples (Supplementary Table 1) were analysed at the Department of Geology, University of Tartu, Estonia, using a Thermo Scientific Delta V Advance continuous flow isotope ratio mass spectrometer and a GasBench II preparation line connected to a Delta V Advantage IRMS (Thermo Fisher Scientific). The carbonate samples were reacted with orthophosphoric acid overnight (>8 h) at 70°C to allow a complete reaction. The results of the carbonate mineral analyses are given in Supplementary Table 1 and are expressed in per mille (‰) deviation relative to the Vienna PeeDee Belemnite (VPDB) scale for oxygen ($\delta^{18}O_{carb}$) and carbon ($\delta^{13}C_{carb}$). Long-term reproducibility is better than ±0.2‰ (2σ) for both the $\delta^{18}O_{carb}$ and $\delta^{13}C_{carb}$ values.

Results

Petrological analysis

The interpreted peak mineral assemblage of the metapelite sample is kyanite + biotite + plagioclase + quartz + rutile + muscovite. This field occurs on the *P–T* diagram (Fig. 3) at 6–10 kbar and 620–670°C, constrained by the presence of melt up temperature, sillimanite-in down pressure, staurolite-in down temperature and paragonite-in up pressure. The low abundance of muscovite in the sample means that *P–T* conditions may correspond to the lowest

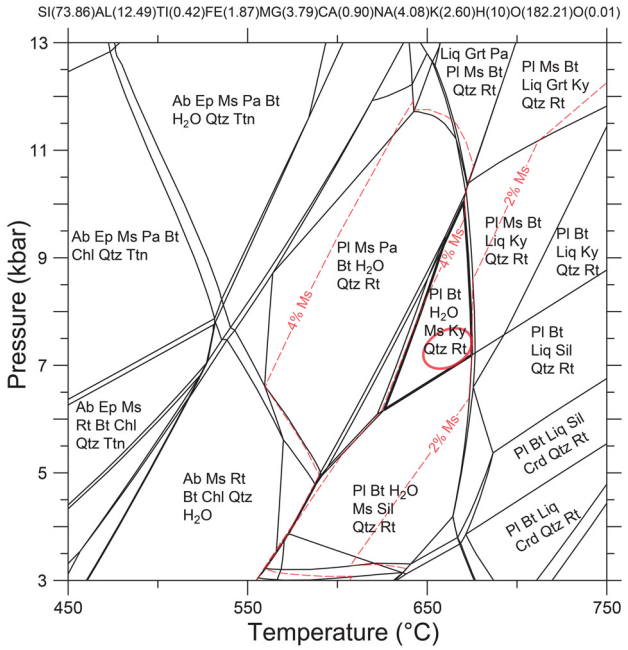

Fig. 3. *P–T* diagram for sample RS-23-08. The interpreted peak assemblage field is highlighted with bold borders. The dashed red lines are vol% contours for muscovite. The red ellipse indicates the part of the field with the lowest amount of white mica, which is likely to correspond to peak conditions for the sample.

muscovite abundance in this field, which occurs in the lower right side (Fig. 3). This indicates peak conditions of 7–8 kbar and 650°C.

U–Pb geochronology

Zircon

Of the 111 zircons analysed, 100 yielded ages that are less than 10% discordant (Fig. 4a). The majority of ages fall in the *c.* 1200–800 Ma range (57 analyses, peaking at 1023 Ma). Subordinate groups are found at *c.* 1711–1586 Ma (13 analyses, peaking at 1620 Ma), *c.* 1512–1437 Ma (nine analyses, peaking at 1489 Ma), *c.* 1388–1249 Ma (13 analyses, peaking at 1350 Ma) and *c.* 763–700 Ma (seven analyses, peaking at 733 Ma). There is also a single Neoarchean age of 2896 Ma.

The zircons in the youngest age group were imaged under CL. They all show evidence of abrasion or breakage (Fig. 4b–d). Many of the zircons (both Neoproterozoic and older) have dark (high-U) rims, and in some cases this high-U zircon phase appears to fill fractures and embayments (Fig. 4b–e). The laser spot avoided these areas because they are too small to give meaningful data, but their internal relationships indicate that they post-date the youngest detrital zircon age.

Monazite

The two monazite grains included in the geochronology programme yielded ages of 441.3 ± 10.2 and 427.9 ± 9.9 Ma.

Rutile

The rutile dataset comprises results from 82 grains. With the exception of a single anomalous date of *c.* 365 Ma, all analyses fall between *c.* 646 and 422 Ma, with the majority forming a peak at *c.* 439 Ma (Fig. 4f).

C–O isotopes

The C–O isotope data are listed in Supplementary Table 1 and are summarized in Figure 5. The data are separated into three marble groupings: those contained within the Glen Urquhart Complex (Fig. 5a, b); those occurring further NE as isolated lenses within the mapped extent of the Glenfinnan Group (Fig. 5c, d); and those that form xenolithic bodies in the Glen Dessarry and Ardgour (Glen Scaddle) plutons (Fig. 5e; see Figs 1 and 2a for the locations). Eighty-eight per cent of all C isotope data ($\delta^{13}C_{carb}$ VPDB) are between −6 and +6‰, with end-member values of −9 and +8‰ (Fig. 5a, c, e). Eighty-two per cent of all O isotope data ($\delta^{18}O_{carb}$ VPDB) are between −20 and −10‰, with outliers of −22 and −8‰ (Fig. 5a, c, e). As noted above and described more thoroughly below, the Glen Urquhart Complex samples can be arranged into a stratigraphic transect: i.e. younging away from their contact with the migmatitic Glenfinnan Group paragneiss. In the Complex, the Torr Buidhe marble body crops out most extensively and yields an internally consistent trend (Fig. 5b) from low to high $\delta^{13}C$ values: the lowest layers are marked by values between −2 and 0‰ that rise upwards to values between 4 and 6‰.

Although we do not have stratigraphic control (i.e. older to younger trends) for the marble-bearing lenses scattered across the Glenfinnan Group outcrop to the NE of Glen Urquhart (Blairnahenachrie, Kirkton, Rebeg and South Clunes: Fig. 2a), two broad groupings are apparent. C–O isotope data for the South Clunes–Rebeg marbles are typified by overall lower $\delta^{13}C$ and somewhat higher $\delta^{18}O$ values relative to the Blairnahenachrie–Kirkton marbles (Fig. 5c, d). Given that each pairing lies within different parts of the Glenfinnan Group outcrop belt and that each yields a range of C–O isotope data that are similar within, but distinctive between, each pairing, it is plausible that they define two separate marble associations. The C–O isotope data for the Glen Dessarry and Ardgour marble bodies are limited in number but also suggest differentiation into two clusters, with the former marked by lower $\delta^{13}C$ and higher $\delta^{18}O$ values relative to the latter (Fig. 5e).

Regarding C isotope values for those samples, as has been long known (e.g. Rumble 1982; Valley 1986), carbon is well buffered to metamorphic overprinting; hence, any resetting would have been slight and we interpret those as reflecting near-original C isotope compositions. This resilience of C isotopes to metamorphic resetting is hinted at by the fact that the C isotope values of the marble xenoliths in the Glen Dessary and Ardgour plutons overlap entirely (Fig. 5e), with the values for the marbles far from those plutons. Oxygen isotopic composition of the carbonates, however, is more prone to resetting and can be significantly altered in diagenetic–hydrothermal–metamorphic recrystallization processes (Banner and Hanson 1990). This is indicated by variable and occasionally strongly negative $^{18}O_{carb}$ values in studied samples (Fig. 5). Particularly, the samples with the most negative $^{18}O_{carb}$ values can be reasonably interpreted as due to isotopic resetting during emplacement of the adjacent Glen Urquhart serpentinite body. Nevertheless, the negligible co-variance between the C and O isotopes for the South Clunes–Rebeg and Blairnahenachrie–Kirkton marbles (Fig. 5c) gives confidence that $\delta^{13}C_{carb}$ values have not been reset like the oxygen isotopic composition and, hence, can be inferred to record original depositional values.

Discussion

Petrological and geochronological constraints on the depositional age and provenance of the kyanite schist

The peak *P–T* conditions indicated by the overall mineral assemblage in the kyanite schist sample RS-23-08 are 6–10 kbar and 620–670°C, compatible with those of 7 kbar and 650°C

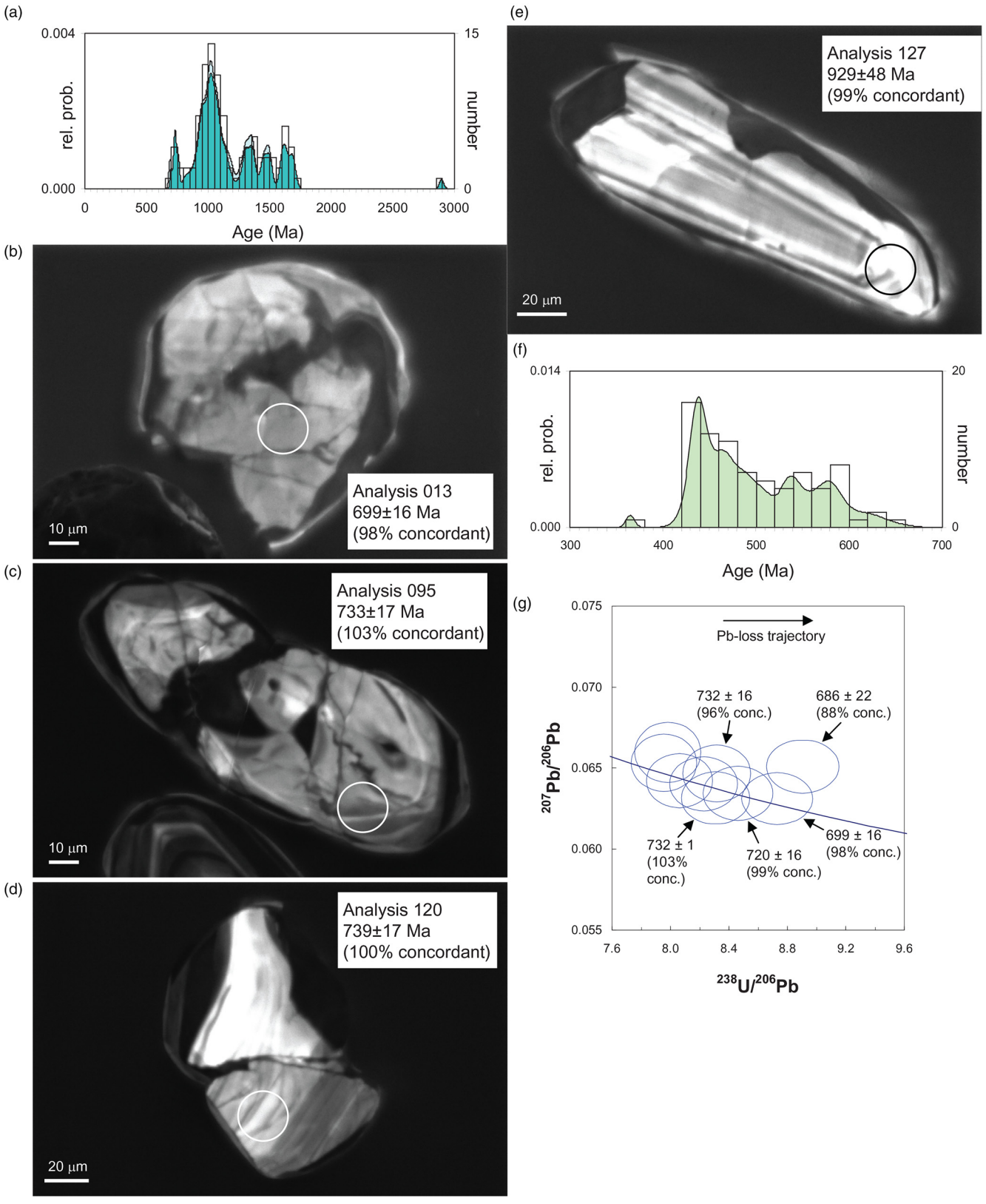

Fig. 4. U–Pb age data and cathodoluminescence (CL) images of selected zircon grains with circles indicating analytical spots. (**a**) Probability density plot of zircon U–Pb ages. The dark green area shows zircons with <10% discordance ($n = 100$); the pale green area is zircons with >10% discordance ($n = 11$). (**b**)–(**d**) CL images of zircons in the youngest age group, all showing evidence of rounding (analyses 13 and 95) or breakage (analysis 120). All three also have dark (high-U) areas that form rims and infill fractures or embayments. (**e**) An older zircon that also has dark (high-U) rims and embayments. (**f**) Probability density plot of rutile U–Pb ages ($n = 82$). (**g**) U–Pb isotopic compositions of the youngest zircon group shown on a Tera–Wasserburg concordia diagram. Data-point ellipses are 2σ.

deduced for Caledonian metamorphism of the host Glenfinnan Group at *c.* 465 Ma (Cutts *et al.* 2010). Taking into account the low abundance of muscovite yields a tighter constraint of 7–8 bar and 650°C (Fig. 3), contrasting with the *P–T* conditions of 9 kbar and 700°C associated with Knoydartian migmatization of the Glenfinnan Group at *c.* 725 Ma (Cutts *et al.* 2010). The difference

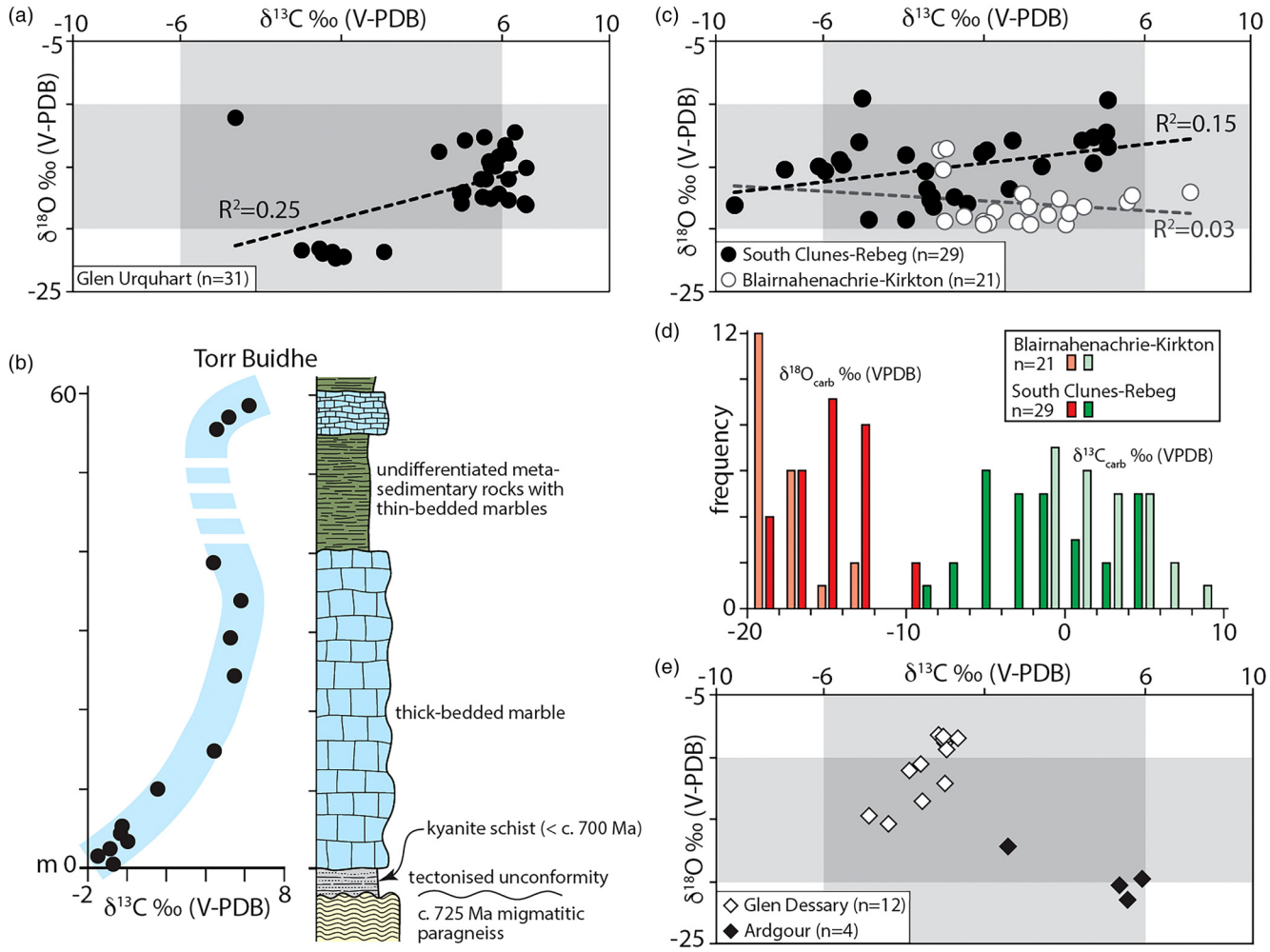

Fig. 5. (**a**) C–O isotope cross-plot of the Glen Urquhart marbles. (**b**) Systematic upward trend defined by the Glen Urquhart marbles. (**c**) C–O isotope cross-plot of the marble lenses that occur as isolated bodies scattered across the Glenfinnan Group outcrop belt. (**d**) Histogram plot of the paired Blairnahenachrie–Kirkton and South Clunes–Rebeg marble localities. (**e**) C–O isotope cross-plot for the Glen Dessarry and Ardgour (Glen Scaddle) xenolithic marble bodies. Note that the lack of co-variance between the C and O isotopes for all data give confidence that the former have not been significantly overprinted by post-depositional processes and hence can be inferred to record original depositional values. See Figures 1 and 2 for the locations.

in these *P–T* conditions is consistent with the hypothesis that the kyanite schist is part of a cover succession that was deposited unconformably on a Glenfinnan Group metasedimentary basement. The absolute difference between the Glenfinnan Group *P–T* conditions is only 1–2 kbar and 50°C; this means that the *P–T* conditions are potentially within error. However, the *P–T* estimate for the *c.* 725 Ma event obtained by Cutts *et al.* (2010) was a *minimum* estimate for peak conditions, with later garnet growth precluding the preservation of the peak conditions of the 725 Ma event. The absence of melt in the kyanite schist sample could potentially be a result of this sample having a different bulk composition to the Glenfinnan Group migmatites. However, the *P–T* diagram in Figure 3 was created using the bulk composition of the kyanite sample and shows that this sample would certainly have experienced melting if it reached conditions of 9 kbar and 700 C, with melt modes indicating 10 vol% melt at these conditions. This amount of melt would be apparent in the sample. Thus, the simplest explanation is that the kyanite schist did not experience the high-grade event at 725 Ma, and the metamorphism apparent in this sample is the result of the 7 kbar and 650°C Caledonian event.

The U–Pb analyses of detrital zircons from the kyanite schist provide important constraints on the depositional age of the sedimentary protolith. The youngest significant age cluster in the dataset is *c.* 760–700 Ma (Fig. 4), with the youngest individual near-concordant analysis being 699.1 ± 15.8 Ma, 2% discordance (2σ errors). However, the use of individual ages to constrain maximum depositional ages (MDAs) is fraught with uncertainty (Coutts *et al.* 2019), especially since it is difficult to detect disturbances of U–Pb systematics (e.g. Pb loss) of zircons with late Neoproterozoic apparent ages owing to the Pb-loss trajectory running near-parallel to the concordia line (Fig. 4g). A more reliable estimate of the MDA for the kyanite schist is afforded by the three analyses of 732.6 ± 16.9, 731.9 ± 16.8 and 720.1 ± 16.6 Ma, which are within 2σ error, and yield an MDA of *c.* 728 Ma. This age is within error identical to the timing of Knoydartian migmatization within the Glenfinnan Group, which we interpret as the source of the youngest detrital zircon grains within the kyanite schist. All of the zircons in the youngest group show evidence of rounding and/or breakage, and have evidently undergone sedimentary transport prior to deposition (Fig. 4). The older zircon grains in the *c.* 760–720 Ma age group could have been derived from a range of Wester Ross Supergroup and Loch Ness Supergroup units that were affected by several episodes of Knoydartian amphibolite-facies metamorphism and pegmatite segregation during that period (Rogers *et al.* 1998; Highton *et al.* 1999; Cawood *et al.* 2015). The youngest detrital zircon grains within the kyanite schist thus support the hypothesis that it was deposited unconformably on Glenfinnan Group metasedimentary basement.

Mesoproterozoic ages clustering at *c.* 1620, 1489, 1350 and 1023 Ma defined by analyses of detrital zircons from the kyanite

schist (Fig. 4a) are consistent with ultimate derivation from various early–mid-Mesoproterozoic accretionary orogens such as the Pinwarian and Elzeverian in North America and the Gothian belt in Baltica, and the end Mesoproterozoic Grenville–Sveconorwegian orogen (Cawood *et al.* 2007*b*; Olierook *et al.* 2020; Bingen *et al.* 2021). However, similar age clusters are recorded in the Glenfinnan Group (Kirkland *et al.* 2008; Cawood *et al.* 2015) and hence much of the more than 1.0 Ga detrital zircon load within the kyanite schist may have been recycled from this and other Tonian supracrustal successions.

C isotope constraints on the age of the marbles and possible regional correlations

Our petrological, geochronological and isotopic data are consistent with the marbles and associated lithologies representing a single succession that was deposited unconformably on the Loch Ness Supergroup. Both units were then isoclinally interfolded and recrystallized at mid-amphibolite facies during the Caledonian Orogeny. This basement–cover relationship is most extensively developed in the Glen Urquhart Complex (Fig. 2b), where the stratigraphic succession above the unconformity is therefore: kyanite schist (oldest), marbles (intermediate in age) and undifferentiated metasediments (youngest). As detailed above, the MDA for this succession identified on the basis of the youngest detrital zircons is *c.* 728 Ma. However, as migmatization of the underlying paragneiss occurred at 725 Ma, a reasonable amount of time had to pass for exhumation of these rocks, and their subsequent erosion followed by deposition and lithification of the sedimentary package that formed the protoliths of the schist–marble succession. Accordingly, we suggest that the Glen Urquhart and associated marbles are likely to be younger than *c.* 700 Ma, which places their deposition between the Cryogenian and the oldest well-constrained ages for its metamorphism, which is Caledonian orogenesis at *c.* 475 Ma (Bird *et al.* 2013; Mako *et al.* 2021).

Accepting those age constraints on the timing of deposition, we then investigated if the C isotopic compositions of the marbles were compatible with the known global carbonate C isotope curve for Cryogenian–early Ordovician time: i.e. the time window our new data indicate as permissible for deposition of the Glen Urquhart and associated marble bodies. As shown by independent assessment of many Neoproterozoic successions worldwide via robust U–Pb and Re–Os geochronology combined with $^{87}Sr/^{86}Sr$ trends, C isotope curves afford a viable method for establishing a proxy age control and aiding correlations between successions both intra- and inter-regionally (e.g. Brasier and Shields 2000; Macdonald *et al.* 2010; Rooney *et al.* 2015, 2020; Fairchild *et al.* 2018; Halverson *et al.* 2020; Zhou *et al.* 2020; Shields *et al.* 2022; Bowyer *et al.* 2025; Yang *et al.* 2025). Figure 6 compares the global C isotope trend with the permissibly equivalent carbonate rocks of the Scottish Highlands: namely, the Argyll Group through to the Trossachs/Clift Hills groups of the Dalradian Supergroup and the Cambrian–Ordovician Durness Group. We note that Rock *et al.* (1984), relying on major and trace element data, rejected correlation of the Glen Urquhart and associated marbles with Dalradian carbonate rock units, but their analysis only evaluated potential linkages with the Appin Group in any detail. Our findings, including the new U–Pb geochronology and showing that the marble–schist packages are autochthonous, not allochthonous, reopen this possibility and make these dismissals equivocal. Any proposed correlation between the Glen Urquhart and associated marbles with units in the Dalradian succession must exhibit both: (i) facies characteristics typified by decimetre- to a-few-tens-of-metre-scale interbedding between carbonate rocks and mostly fine-grained siliciclastic rocks (i.e. comparable to the Glen Urquhart schist–marble–psammite succession); and (ii) compatible C isotope values (i.e. mostly between −6 and +6‰ with rare outliers to *c.* −9 or +8‰) within a narrow stratigraphic distribution. Given these

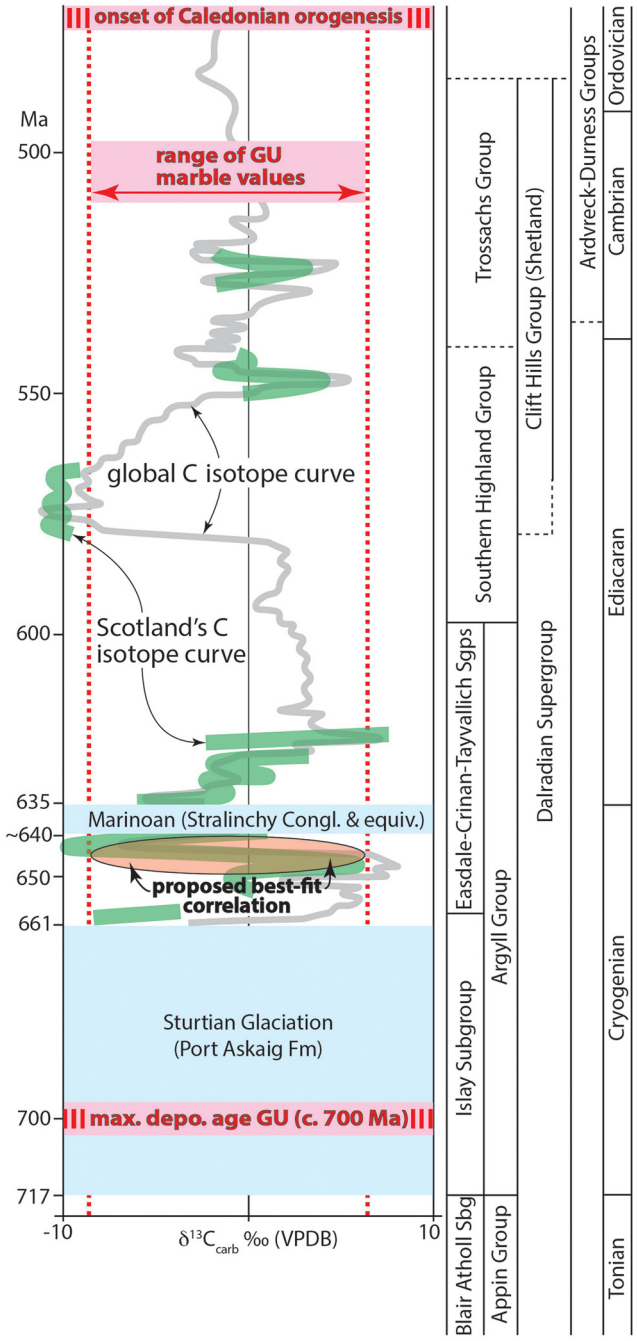

Fig. 6. Plot of the global average trend of carbonate C isotopes ($\delta^{13}C_{carb}$) for late Tonian–early Ordovician time with the trend of the time-equivalent Dalradian Supergroup C isotope record superimposed on the global curve. The currently accepted ages for the Cryogenian global glaciations are listed. The vertical dashed red lines denote the range in C isotope values exhibited by the Glen Urquhart and associated marbles (GU). The red ellipse is our interpretation of their best-fit correlation with the Dalradian succession. Source: data for the carbonate C isotopes are from Halverson *et al.* (2020) and data for the Dalradian Supergroup C isotope record are from Prave *et al.* (2024*a* and references therein).

criteria, Ediacaran and Cambro-Ordovician carbonate rocks in the Scottish Highlands can be ruled out as potential correlatives in that the former are associated with thick successions of deep-water (commonly turbiditic) psammitic/semi-pelitic and volcanic rocks, and the latter comprises a succession of limestones/dolostones many hundreds of metres thick. Consequently, we conclude that the best-fit correlatives for the Glen Urquhart marbles and those forming the two infolded bands in the Glenfinnan Group are the Easdale Subgroup limestones (Fig. 6).

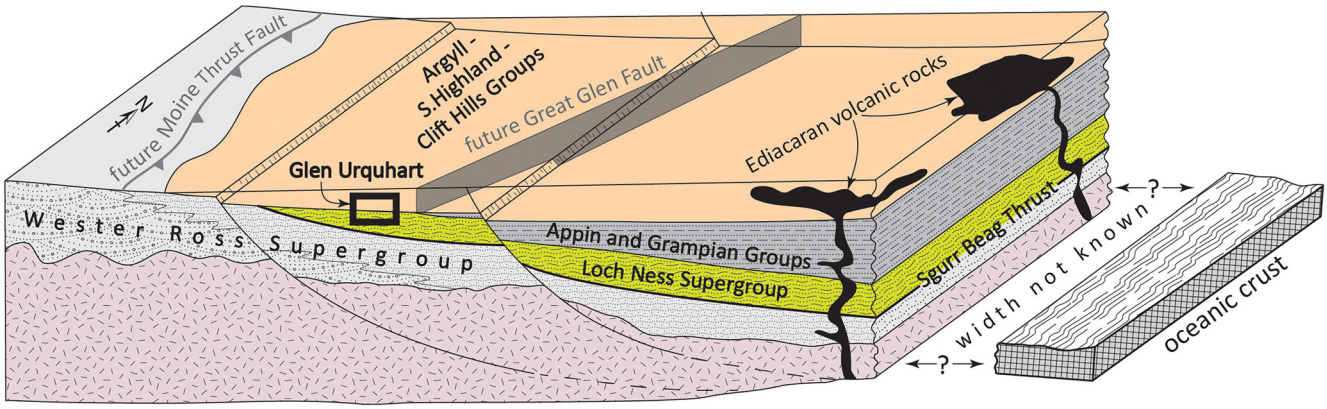

Fig. 7. Schematic cross-section of the Laurentian continental margin during late Ediacaran time, showing the inferred location of the autochthonous Glen Urquhart kyanite schist–marble association, which in this diagram also includes the marble bodies now occurring as scattered dismembered lenses within the Glenfinnan Group outcrop belt. We interpret the Wester Ross and Loch Ness supergroups as a composite metasedimentary basement (deformed and metamorphosed during Tonian orogenies) that was downwarped and then buried by Dalradian successions. The oldest of these are the foreland and successor basin successions of the late Tonian Grampian–Appin groups. Subsequent rifting during the Cryogenian–early Ordovician generated accommodation space for the rift–post-rift–early passive margin successions of the Argyll–Southern Uplands groups on the Scottish mainland and equivalent Clift Hills Group in Shetland. Note the progressive northwestward onlap of these successions across the Great Glen Fault (GGF).

Regional depositional setting and tectonic framework

A simplified reconstruction of the Laurentian passive continental margin depicts the main Neoproterozoic stratigraphic units in their likely relative positions during late Cryogenian–Ediacaran time (Fig. 7). This assumes that subsequent Caledonian displacements along the Sgurr Beag and Moine thrusts and the GGF were significantly smaller in scale than the overall dimensions of the continental margin (Krabbendam *et al.* 2021; Prave *et al.* 2024*b*). We suggest that deposition of the Grampian and Appin groups was restricted to east of the precursor of the GGF, but the Dalradian sedimentary basin subsequently widened so that strata of the Argyll–Southern Highland groups progressively onlapped northwestwards. This explains the deposition of Argyll Group-equivalent strata unconformably on the metamorphic basement of the Loch Ness Supergroup. Deposition of these strata on the Glenfinnan Group adjacent to the GGF is likely to reflect marked eastward thinning of the Loch Eil Group (Strachan *et al.* 1988), although deposition on the overturned upper limb of a large-scale pre-Caledonian (Knoydartian) fold cannot be ruled out.

Continued extension and subsidence of the passive margin during the Cambrian–early Ordovician resulted in deposition on the Hebridean foreland of the Ardvreck and Durness groups, which were temporally equivalent to the uppermost parts of the Dalradian Supergroup, and the Southern Highland and Trossachs groups in the region of the Highland Boundary Fault (Fig. 1) (Prave *et al.* 2024*a*). However, these successions are likely to have been supplied detritus from different source regions. Detrital zircons were delivered to the Hebridean foreland from the NW, possibly Greenland, whereas the upper Dalradian units derived detritus from source regions to the SW such as NE Canada and/or recycling of the Loch Ness Supergroup (Cawood *et al.* 2007*a*, 2012).

Implications for the ages of tectonic structures

The demonstration of a tectonized unconformity within this tract of high-grade metamorphic rocks in the Scottish Caledonides provides an important means of constraining the ages of tectonic structures. If the Glen Urquhart kyanite schist–marble succession is mid-Cryogenian in age, all structures that have affected it must have formed during the Caledonian Orogeny, namely the D_2 and D_3 folds and associated structures. These would, of course, be the first and second structures to affect these rocks, and so could be referred to as D_1 and D_2 if only the kyanite schist–marble association was being considered. In the absence of any evidence to the contrary, the D_2 folds and associated structures are assumed to have formed at *c.* 470–465 Ma, coeval with the timing of high-grade metamorphism (Cutts *et al.* 2010; Bird *et al.* 2013; Mako *et al.* 2021). If a late-D_2 age of emplacement for the serpentinite can be substantiated, this suggests potential affinities with *c.* 470 Ma metagabbros that intrude the Dalradian Supergroup in NE Scotland (Stephenson *et al.* 1999; Leslie *et al.* 2024 and references therein). The *c.* 440 and *c.* 427 Ma monazite and rutile ages obtained from the kyanite schist are most likely to have recorded a younger Caledonian metamorphic event that was broadly coeval with D_3 upright folding. Monazite and rutile have relatively high closure temperatures of at least 700 and *c.* 600°C, respectively (Cherniak 2000; Vry and Baker 2006); hence, these ages are unlikely to record cooling following the earlier high-grade metamorphic event. The high-U zircon rims and fracture fills seen on many of the zircon grains are attributed to hydrothermal/metasomatic zircon growth during the Caledonian Orogeny.

Conclusions

(1) Structural analysis indicates that: (a) there is no evidence that the Glen Urquhart kyanite schist–marble succession is allochthonous; and (b) the serpentinite body is likely to have been intruded after the host metasediments had undergone tight to isoclinal folding and kyanite-grade metamorphism. The term ‘Glen Urquhart Complex’ carries the connotation that the two units are temporally and/or generically related in some way but should now be abandoned.

(2) Petrological analysis indicates a clear difference between peak metamorphic conditions for the Glen Urquhart kyanite schist (7–8 kbar and 650°C at 475–465 Ma) and the adjacent Glenfinnan Group paragneisses (9 kbar and 700°C at *c.* 725 Ma).

(3) Detrital zircons from the Glen Urquhart kyanite schist yield a range of Paleoproterozoic–mid-Neoproterozoic U–Pb ages, consistent with ultimate derivation from various circum-Atlantic crustal blocks. The most reliable estimate of the maximum depositional age based on the zircon data alone is *c.* 728 Ma, which overlaps with the age of migmatization of the adjacent Glenfinnan Group paragneisses (Cutts *et al.* 2010). However, in order to

provide sufficient time for the exhumation of the paragneisses, their subsequent erosion, and deposition and lithification of the sedimentary protoliths of the kyanite schist–marble succession, the latter is likely to be younger than 700 Ma.

(4) Petrological and geochronological data thus indicate that the contact between the Glen Urquhart kyanite schist–marble succession and adjacent Glenfinnan Group paragneisses is a tectonically modified unconformity.

(5) C–O isotope data are consistent with a late Cryogenian age for the Glen Urquhart marbles and other isolated marble occurrences within the Loch Ness Supergroup. We correlate these marbles with those in the Easdale Subgroup (Dalradian Supergroup) east of the GGF. We suggest that deposition of the lower Grampian and Appin groups of the Dalradian Supergroup was restricted to east of the precursor of the GGF, but the Dalradian sedimentary basin subsequently widened so that strata of the Argyll–Southern Highland groups progressively onlapped northwestwards and were deposited unconformably on the Loch Ness Supergroup.

(6) All structures that affect the Glen Urquhart kyanite schist–marble succession must have formed during the Caledonian Orogeny, namely the D_2 and D_3 folds and associated structures. The D_2 folds are assumed to have formed at *c.* 475–465 Ma, coeval with the timing of high-grade metamorphism (Cutts *et al.* 2010; Bird *et al.* 2013; Mako *et al.* 2021). U–Pb ages of *c.* 440–428 Ma obtained from monazite and rutile are likely to correspond to the timing of D_3 folding.

(7) This case study presents the first unequivocal evidence for a basement–cover relationship within the high-grade internal zone of the Scottish Caledonides north of the GGF, and demonstrates the utility of a multidisciplinary approach in identifying orogenic unconformities that have been overprinted by intense ductile deformation and amphibolite-facies metamorphism.

Scientific editing by Yildirim Dilek

Acknowledgements We thank David Chew for a detailed review and Yildirim Dilek for efficient editorial handling.

Author contributions **RAS**: conceptualization (equal), formal analysis (equal), investigation (equal), writing – original draft (equal), writing – review & editing (equal); **ARP**: conceptualization (equal), formal analysis (equal), investigation (equal), writing – original draft (equal), writing – review & editing (equal); **AM**: formal analysis (equal), investigation (equal), writing – original draft (supporting), writing – review & editing (supporting); **DF**: formal analysis (equal), investigation (equal), writing – original draft (supporting), writing – review & editing (supporting); **KK**: formal analysis (equal), investigation (equal), writing – original draft (supporting), writing – review & editing (supporting); **KAC**: formal analysis (equal), investigation (equal), writing – original draft (supporting), writing – review & editing (supporting).

Funding This research received no specific grant from any funding agency in the public, commercial, or not-for-profit sectors.

Competing interests The authors declare that they have no known competing financial interests or personal relationships that could have appeared to influence the work reported in this paper.

Data availability All data generated or analysed during this study are included in this published article (and if present, its supplementary information files).

References

Aftalion, M., Bowes, D.R. and V?ana, S. 1989. Early Carboniferous U–Pb zircon ages for garnetiferous perpotassic granulites, Blanský les massif, Czechoslovakia. *Neues Jahrbuch für Mineralogie, Monatshefte*, **4**, 145–152.

Aleinikoff, J.N., Schenck, W.S., Srogi, L.A., Fanning, C.M., Kamo, S.L. and Bosbyshell, H. 2006. Deciphering igneous and metamorphic events in high-grade rocks of the Wilmington Complex, Delaware: Morphology, cathodoluminescence and backscattered electron zoning, and SHRIMP U–Pb geochronology of zircon and monazite. *Geological Society of America Bulletin*, **118**, 39–64, https://doi.org/10.1130/B25659.1

Banner, J.L. and Hanson, G.N. 1990. Calculation of simultaneous isotopic and trace element variations during water–rock interaction with applications to carbonate diagenesis. *Geochimica et Cosmochimica Acta*, **54**, 3123–3137, https://doi.org/10.1016/0016-7037(90)90128-8

Bingen, B., Viola, G., Möller, C., Vander Auwera, J., Laurent, A. and Keewook, Y. 2021. The Sveconorwegian Orogeny. *Gondwana Research*, **90**, 273–313, https://doi.org/10.1016/j.gr.2020.10.014

Bird, A.F., Thirlwall, M.F. and Strachan, R.A. 2013. Lu–Hf and Sm–Nd dating of metamorphic garnet: evidence for multiple accretion events during the Caledonian orogeny in Scotland. *Journal of the Geological Society, London*, **170**, 301–317, https://doi.org/10.1144/jgs2012-083

Bird, A.F., Cutts, K.A., Strachan, R.A., Thirlwall, M.F. and Hand, M. 2018. First evidence of Renlandian (c. 950–940 Ma) orogeny in Mainland Scotland: Implications for the status of the Moine Supergroup and circum-North Atlantic correlations. *Precambrian Research*, **305**, 293–294, https://doi.org/10.1016/j.precamres.2017.12.019

Bowyer, F.T., Messori, F. *et al.*. 2025. Foundational uncertainties in terminal Ediacaran chronostratigraphy revealed by high-precision zircon U–Pb geochronology of the Nama Group, Namibia. *Earth-Science Reviews*, **268**, https://doi.org/10.1016/j.earscirev.2025.105169

Brasier, M.D. and Shields, G. 2000. Neoproterozoic chemostratigraphy and correlation of the Port Askaig glaciation, Dalradian Supergroup of Scotland. *Journal of the Geological Society, London*, **157**, 909–914, https://doi.org/10.1144/jgs.157.5.909

British Geological Survey 2007. *Bedrock Geology UK North, 1:625 000 Scale*, 5th edn. British Geological Survey (BGS), Keyworth, Nottingham, UK.

Capitani, C.de and Petrakakis, K. 2010. The computation of equilibrium assemblage diagrams with Theriak/Domino software. *American Mineralogist*, **95**, 1006–1016, https://doi.org/10.2138/am.2010.3354

Cawood, P.A., Nemchin, A.A., Strachan, R.A., Kinny, P.D. and Loewy, S. 2004. Laurentian provenance and an intracratonic setting for the Moine Supergroup, Scotland, constrained by detrital zircons from the Loch Eil and Glen Urquhart successions. *Journal of the Geological Society, London*, **161**, 861–874, https://doi.org/10.1144/16-764903-117

Cawood, R.A., Nemchin, A.A. and Strachan, R.A. 2007*a*. Provenance record of Laurentian passive margin strata in the northern Caledonides: Implications for paleodrainage and paleogeography. *Geological Society of America Bulletin*, **119**, 993–1003, https://doi.org/10.1130/B26152.1

Cawood, P.A., Nemchin, A.A., Strachan, R.A., Prave, A.R. and Krabbendam, M. 2007*b*. Sedimentary basin and detrital zircon record along East Laurentia and Baltica during assembly and breakup of Rodinia. *Journal of the Geological Society, London*, **164**, 257–275, https://doi.org/10.1144/0016-76492006-115

Cawood, P.A., Strachan, R.A., Cutts, K.A., Kinny, P.D., Hand, M. and Pisarevsky, S. 2010. Neoproterozoic orogeny along the margin of Rodinia: Valhalla orogen, North Atlantic. *Geology*, **38**, 99–102, https://doi.org/10.1130/G30450.1

Cawood, P.A., Merle, R.E., Strachan, R.A. and Tanner, P.W.G. 2012. Provenance of the Highland Border Complex: constraints on Laurentian margin accretion in the Scottish Caledonides. *Journal of the Geological Society, London*, **169**, 575–586, https://doi.org/10.1144/0016-76492011-076

Cawood, P.A., Strachan, R.A. *et al.* 2015. Neoproterozoic to early Palaeozoic extensional and contractional history of East Laurentian margin sequences. The Moine Supergroup, Scottish Caledonides. *Geological Society of America Bulletin*, **127**, 349–371, https://doi.org/10.1130/B31068.1

Cherniak, D.J. 2000. Pb diffusion in rutile. *Contributions to Mineralogy and Petrology*, **139**, 198–207, https://doi.org/10.1007/PL00007671

Cornell, D.H., Zack, T., Andersen, T., Corfu, F., Frei, D. and Van Schijndel, V. 2016. Th–U–Pb zircon geochronology of the Palaeoproterozoic Hartley Formation porphyry by six methods, with age uncertainty approaching 1 Ma. *South African Journal of Geology*, **119**, 473–494, https://doi.org/10.2113/gssajg.119.3.473

Couëslan, C.G., Pattison, D.R.M. and Dufrane, S.A. 2013. Paleoproterozoic metamorphic and deformation history of the Thompson Nickel Belt, Superior Boundary Zone, Canada, from in situ U–Pb analysis of monazite. *Precambrian Research*, **237**, 13–35, https://doi.org/10.1016/j.precamres.2013.06.009

Coutts, D.S., Matthews, W.A. and Hubbard, S.M. 2019. Assessment of widely used methods to derive depositional ages from detrital zircon populations. *Geoscience Frontiers*, **10**, 1421–1435, https://doi.org/10.1016/j.gsf.2018.11.002

Cutts, K.A., Hand, M., Kelsey, D.E., Wade, B., Strachan, R.A., Clark, C. and Netting, A. 2009. Evidence for 930 Ma metamorphism in the Shetland Islands, Scottish Caledonides: implications for Neoproterozoic tectonics in the the Laurentia–Baltica sector of Rodinia. *Journal of the*

Geological Society, London, **166**, 1033–1048, https://doi.org/10.1144/0016-76492009-006

Cutts, K.A., Kinny, P.D. *et al.* 2010. Three metamorphic events recorded in a single garnet: coupled phase modelling with in situ LA-ICPMS, and SIMS geochronology from the Moine Supergroup, NW Scotland. *Journal of Metamorphic Geology*, **28**, 249–267, https://doi.org/10.1111/j.1525-1314.2009.00863.x

Drever, H.I. 1940. The geology of Ardgour, Argyllshire. *Transactions of the Royal Society of Edinburgh*, **60**, 141–171, https://doi.org/10.1017/S0080456800017853

Emery, M.R.G. 2005. *Poly-Orogenic History of the Moine Rocks of Glen Urquhart, Eastern Inverness-Shire*. PhD thesis, University of Portsmouth, Portsmouth, UK.

Fairchild, I.J., Spencer, A.M. *et al.* 2018. Tonian–Cryogenian boundary sections Argyll, Scotland. *Precambrian Research*, **319**, 37–64, https://doi.org/10.1016/j.precamres.2017.09.020

Francis, G.H. 1956. The serpentinite mass in Glen Urquhart, Inverness-shire, Scotland. *American Journal of Science*, **254**, 201–226, https://doi.org/10.2475/ajs.254.4.201

Francis, G.H. 1958. Petrological studies in Glen Urquhart, Inverness-shire. *Bulletin of the British Museum (Natural History), Minerals*, **1**, 123–154, https://www.biodiversitylibrary.org/page/41132488

Francis, G.H. 1964. Further petrological studies in Glen Urquhart, Inverness-shire. *Bulletin of the British Museum (Natural History), Minerals*, **1**, 165–199, https://www.biodiversitylibrary.org/page/41129691

Frei, D. and Gerdes, A. 2009. Precise and accurate *in situ* U–Pb dating of zircon with high sample throughput by automated LA-SF-ICPMS. *Chemical Geology*, **261**, 261–270, https://doi.org/10.1016/j.chemgeo.2008.07.025

Gerdes, A. and Zeh, A. 2006. Combined U–Pb and Hf isotope LA-(MC)-ICP-MS analyses of detrital zircons: Comparison with SHRIMP and new constraints for the provenance and age of an Armorican metasediment in Central Germany. *Earth and Planetary Science Letters*, **249**, 47–61, https://doi.org/10.1016/j.epsl.2006.06.039

Goodenough, K.M., Millar, I., Strachan, R.A., Krabbendam, M. and Evans, J.A. 2011. Timing of regional deformation and development of the Moine Thrust Zone in the Scottish Caledonides, constraints from the U–Pb geochronology of alkaline intrusions. *Journal of the Geological Society, London*, **168**, 99–114, https://doi.org/10.1144/0016-76492010-020

Halverson, G.P., Porter, S. and Shields, G. 2020. The Tonian and Cryogenian periods. *In*: Gradstein, F.M., Ogg, J.G., Schmitz, M.D. and Ogg, G.M. (eds) *Geologic Time Scale 2020, Volume 1*. Elsevier, Amsterdam, 495–519, https://doi.org/10.1016/B978-0-12-824360-2.00017-6

Harry, W.T. 1951. The migmatites and felspar porphyroblast rock of Glen Dessary, Inverness-shire. *Quarterly Journal of the Geological Society, London*, **107**, 137–158, https://doi.org/10.1144/GSL.JGS.1951.107.01-04.06

Heptinstall, E. 2025. Unusual Scottish marbles of The Aird. *The Edinburgh Geologist*, **78**, 6–13, https://edinburghgeolsoc.org/eg_pdfs/edinburgh-geologist-78.pdf

Highton, A.J., Hyslop, E.K. and Noble, S.R. 1999. U–Pb zircon geochronology of migmatization in the northern Central Highlands: evidence for pre-Caledonian (Neoproterozoic) tectonometamorphism in the Grampian Block, Scotland. *Journal of the Geological Society, London*, **156**, 1195–1204, https://doi.org/10.1144/gsjgs.156.6.1195

Holdsworth, R.E., Strachan, R.A. and Harris, A.L. 1994. Precambrian rocks in northern Scotland east of the Moine Thrust: the Moine Supergroup. *Geological Society, London, Special Report*, **22**, 23–32, https://doi.org/10.1144/SR22.3

Holland, T. and Powell, R. 2003. Activity–composition relations for phases in petrological calculations: an asymmetric multicomponent formulation. *Contributions to Mineralogy and Petrology*, **145**, 492–501, https://doi.org/10.1007/s00410-003-0464-z

Holland, T.J.B. and Powell, R. 2011. An improved and extended internally consistent thermodynamic dataset for phases of petrological interest, involving a new equation of state for solids. *Journal of Metamorphic Geology*, **29**, 333–383, https://doi.org/10.1111/j.1525-1314.2010.00923.x

Horne, J. and Hinxman, L.W. 1914. *The Geology of the Country around Beauly and Inverness. Explanation of Sheet 83*. Memoirs of the British Geological Survey. HM Stationery Office, Edinburgh.

Janoušek, V. and Gerdes, A. 2003. Timing the magmatic activity within the Central Bohemian Pluton, Czech Republic: conventional U–Pb ages for the Sázava and Tábor intrusions and their geotectonic significance. *Journal of the Czech Geological Society*, **48**, 70–71.

Jørgensen, T.R.C., Tinkham, D.K. and Lesher, C.M. 2019. Low-*P* and high-*T* metamorphism of basalts: Insights from the Sudbury impact melt sheet aureole and thermodynamic modelling. *Journal of Metamorphic Geology*, **37**, 271–313, https://doi.org/10.1111/jmg.12460

Kinny, P.D., Strachan, R.A. *et al.* 2025. Early Neoproterozoic (Tonian) subduction-related magmatism and tectonothermal activity in Shetland and northern mainland Scotland: implications for the tectonic evolution of northeast Laurentia, and Rodinia reconstructions. *Journal of the Geological Society, London*, **181**, https://doi.org/10.1144/jgs2024-093

Kirkland, C.L., Strachan, R.A. and Prave, A.R. 2008. Detrital zircon signature of the Moine Supergroup, Scotland: Contrasts and comparisons with other Neoproterozoic successions within the circum-North Atlantic region. *Precambrian Research*, **163**, 332–350, https://doi.org/10.1016/j.precamres.2008.01.003

Krabbendam, M., Strachan, R.A. and Prave, A.R. 2021. A new stratigraphic framework for the early Neoproterozoic successions of NW Scotland. *Journal of the Geological Society, London*, **177**, https://doi.org/10.1144/jgs2021-054

Lambert, R.StJ., Poole, A.B., Richardson, S.W., Johnstone, G.S. and Smith, D.I. 1964. The Glen Dessarry syenite, Inverness-shire. *Nature*, **202**, 370–372, https://doi.org/10.1038/202370a0

Lanari, P., Vidal, O., De Andrade, V., Dubacq, B., Lewin, E., Grosch, E.G. and Schwartz, S. 2014. XMapTools: A MATLAB©-based program for electron microprobe X-ray image processing and geothermobarometry. *Computing Geoscience*, **62**, 227–240, https://doi.org/10.1016/j.cageo.2013.08.010

Law, R.D., Strachan, R.A., Thirlwall, M. and Thigpen, J.R. 2024. The Caledonian Orogeny: Late Ordovician–Early Devonian tectonic and magmatic events associated with closure of the Iapetus Ocean. *In*: Smith, M. and Strachan, R.A. (eds) *The Geology of Scotland*. 5th edn. Geological Society, London, 205–257, https://doi.org/10.1144/GOS5-2022-71

Leslie, A.G., Stone, P. and Strachan, R.A. 2024. Early–Middle Ordovician Grampian orogenesis: ophiolite obduction and arc–continent collision. *In*: Smith, M. and Strachan, R.A. (eds) *The Geology of Scotland*. 5th edn. Geological Society, London, 139–170, https://doi.org/10.1144/GOS5-2021-42

Ludwig, K. 2003. *Isoplot/Ex Version 3: A Geochronological Toolkit for Microsoft Excel*. Geochronology Center, Berkeley, CA.

Luvizotto, G.L., Zack, T. *et al.* 2009. Rutile crystals as potential trace element and isotope mineral standards for microanalysis. *Chemical Geology*, **261**, 346–369, https://doi.org/10.1016/j.chemgeo.2008.04.012

Macdonald, F.A., Schmitz, M.D. *et al.* 2010. Calibrating the Cryogenian. *Science*, **327**, 1241–1243, https://doi.org/10.1126/science.1183325

Mako, C.A., Law, R.D. *et al.* 2021. Growth and fluid-assisted alteration of accessory phases before, during and after Rodinia break-up: U–Pb geochronology from the Moine Supergroup rocks of northern Scotland. *Precambrian Research*, **355**, https://doi.org/10.1016/j.precamres.2020.106089

Mattinson, J.M. 2010. Analysis of the relative decay constants of ^{235}U and ^{238}U by multi-step CA-TIMS measurements of closed-system natural zircon samples. *Chemical Geology*, **275**, 186–198, https://doi.org/10.1016/j.chemgeo.2010.05.007

Nasdala, L., Hofmeister, W. *et al.* 2008. Zircon M257 – a homogeneous natural reference material for the ion microprobe U–Pb analysis of zircon. *Geostandards and Geoanalytical Research*, **32**, 247–265, https://doi.org/10.1111/j.1751-908X.2008.00914.x

Olierook, H.K.H., Barham, M., Kirkland, C.L., Hollis, J. and Vass, A. 2020. Zircon fingerprint of the Neoproterozoic North Atlantic: Perspectives from East Greenland. *Precambrian Research*, **342**, https://doi.org/10.1016/j.precamres.2020.105653

Prabhakar, N. 2013. Resolving poly-metamorphic Paleoarchean ages by chemical dating of monazites using multi-spectrometer U, Th and Pb analyses and sub-counting methodology. *Chemical Geology*, **347**, 255–270, https://doi.org/10.1016/j.chemgeo.2013.04.012

Prave, A.R., Fallick, A.E. and Kirsimäe, K. 2023. Evidence, or not, for the late Tonian break-up of Rodinia? The Dalradian Supergroup of Scotland. *Journal of the Geological Society, London*, **180**, https://doi.org/10.1144/jgs2022-134

Prave, A.R., Fallick, A.E., Strachan, R.A., Krabbendam, M. and Leslie, A.G. 2024*a*. Middle Neoproterozoic–Early Ordovician: foreland basins, climatic extremes and rift-to-drift margins. *In*: Smith, M. and Strachan, R.A. (eds) *The Geology of Scotland*. 5th edn. Geological Society, London, 111–138, https://doi.org/10.1144/GOS5-2022-12

Prave, A.R., Stephens, W.E., Fallick, A.E., Williams, I.S. and Kirsimäe, K. 2024*b*. How great is the Great Glen Fault? *Journal of the Geological Society, London*, **181**, https://doi.org/10.1144/jgs2024-085

Rock, N.M.S. and Dabek, Z.W. 1990. *A Reappraisal of the Glen Urquhart Serpentinite-Metamorphic Complex and its Moine Envelope, West of Loch Ness*. BGS Technical Report WA/90/72. British Geological Survey (BGS), Edinburgh.

Rock, N.M.S., Jeffreys, L. and MacDonald, R. 1984. The problem of anomalous local limestone–pelite successions within the Moine outcrop; I: metamorphic limestones of the Great Glen area from Ardgour to Nigg. *Scottish Journal of Geology*, **20**, 383–406, https://doi.org/10.1144/sjg20030383

Rock, N.M.S., MacDonald, R., Drewery, S.E., Pankhurst, R.J. and Brook, M. 1986. Pelites of the Glen Urquhart serpentinite–metamorphic complex, west of Loch Ness (anomalous local limestone–pelite successions within the Moine outcrop: III). *Scottish Journal of Geology*, **22**, 179–202, https://doi.org/10.1144/sjg22020179

Rogers, G., Hyslop, E.K., Strachan, R.A., Paterson, B.A. and Holdsworth, R.E. 1998. The structural setting and U–Pb geochronology of Knoydartian pegmatites in W Inverness-shire: evidence for Neoproterozoic tectonothermal events in the Moine of NW Scotland. *Journal of the Geological Society, London*, **155**, 685–696, https://doi.org/10.1144/gsjgs.155.4.0685

Rooney, A.D., Strauss, J., Brandon, A.D. and Macdonald, F. 2015. A Cryogenian chronology: Two long-lasting synchronous Neoproterozoic glaciations. *Geology*, **43**, 459–462, https://doi.org/10.1130/G36511.1

Rooney, A.D., Cantine, M.D. *et al.* 2020. Calibrating the coevolution of Ediacaran life and environment. *Proceedings of the National Academy of*

Sciences of the United States of America, **117**, 16 824–16 830, https://doi.org/10.1073/pnas.2002918117

Rumble, D. 1982. Stable isotope fractionation during metamorphic devolatilization reactions. *Reviews in Mineralogy*, **10**, 327–353.

Russell, M.J., Allison, I., Anderton, R. and Hall, A.J. 1986. Metamorphic limestones of the Great Glen area: comments. *Scottish Journal of Geology*, **22**, 137–139, https://doi.org/10.1144/sjg22010137

Schmitt, A.K. and Zack, T. 2012. High-sensitivity U–Pb rutile dating by secondary ion mass spectrometry (SIMS) with an O_2^+ beam. *Chemical Geology*, **332–333**, 65–73, https://doi.org/10.1016/j.chemgeo.2012.09.023

Shields, G., Strachan, R.A. *et al.* 2022. A template for an improved rock-based subdivision of the pre-Cryogenian timescale. *Journal of the Geological Society, London*, **179**, https://doi.org/10.1144/jgs2020-222

Sircombe, K.N. 2004. AgeDisplay: an EXCEL workbook to evaluate and display univariate geochronological data using binned frequency histograms and probability density distributions. *Computers & Geosciences*, **30**, 21–31, https://doi.org/10.1016/j.cageo.2003.09.006

Sláma, J., Košler, J. *et al.* 2008. Plešovice zircon – a new natural reference material for U–Pb and Hf isotopic microanalysis. *Chemical Geology*, **249**, 1–35, https://doi.org/10.1016/j.chemgeo.2007.11.005

Stephenson, D., Bevins, R.E., Millward, D., Highton, A.J., Parsons, I, Stone, P. and Wadsworth, W.J. 1999. *Caledonian Igneous Rocks of Great Britain*. Geological Conservation Review Series, **17**. Joint Nature Conservation Committee, Peterborough, UK.

Strachan, R.A. and Evans, J.A. 2008. Structural setting and U–Pb zircon geochronology of the Glen Scaddle Metagabbro: evidence for polyphase Scandian ductile deformation in the Caledonides of northern Scotland. *Geological Magazine*, **145**, 361–371, https://doi.org/10.1017/S0016756808004500

Strachan, R.A., May, F. and Barr, D. 1988. The Glenfinnan and Loch Eil divisions of the Moine Assemblage. *In*: Winchester, J.A. (ed.) *Later Proterozoic Stratigraphy of the North Atlantic Region*. Blackie & Sons, Glasgow, UK, 30–45, https://doi.org/10.1007/978-1-4615-7344-9

Strachan, R.A., Prave, A.R., Krabbendam, M. and Smith, M. 2024. Late Mesoproterozoic–middle Neoproterozoic sedimentation and orogeny. *In*: Smith, M. and Strachan, R.A. (eds) *The Geology of Scotland*. 5th edn. Geological Society, London, 81–110, https://doi.org/10.1144/GOS5-2022-14

Valley, J. 1986. Stable isotope geochemistry of metamorphic rocks. *Reviews in Mineralogy*, **16**, 445–489.

van Breemen, O., Aftalion, M., Pankhurst, R.J. and Richardson, S.W. 1979. Age of the Glen Dessary syenite, Inverness-shire: diachronous Palaeozoic metamorphism across the Great Glen. *Scottish Journal of Geology*, **15**, 49–62, https://doi.org/10.1144/sjg15010049

Vry, J.K. and Baker, J.A. 2006. LA-MC-ICPMS Pb–Pb dating of rutile from slowly cooled granulites: Confirmation of the high closure temperature for Pb diffusion in rutile. *Geochimica et Cosmochimica Acta*, **70**, 1807–1820, https://doi.org/10.1016/j.gca.2005.12.006

White, R.W., Powell, R., Holland, T.J.B., Johnson, T.E. and Green, E.C.R. 2014*a*. New mineral activity–composition relations for thermodynamic calculations in metapelitic systems. *Journal of Metamorphic Geology*, **32**, 261–286, https://doi.org/10.1111/jmg.12071

White, R.W., Powell, R. and Johnson, T.E. 2014*b*. The effect of Mn on mineral stability in metapelites revisited: new *a–x* relations for manganese-bearing minerals. *Journal of Metamorphic Geology*, **32**, 809–828, https://doi.org/10.1111/jmg.12095

Wicks, F.J. 1984. Deformation histories as recorded by serpentinites. I. Deformation prior to serpentinization. *Canadian Mineralogist*, **22**, 185–195.

Wiedenbeck, M., Alle, P. *et al.* 1995. Three natural zircon standards for U–Th–Pb, Lu–Hf, trace-element and REE analyses. *Geostandards Newsletter*, **19**, 1–23, https://doi.org/10.1111/j.1751-908X.1995.tb00147.x

Yang, C., Bowyer, F. and Condon, D. 2025. High-precision CA-ID-TIMS zircon U–Pb geochronology: a review of the Neoproterozoic time scale. *National Science Review*, **12**, https://doi.org/10.1093/nsr/nwaf206

Zhou, Y., Pogge von Strandmann, P.A.E. *et al.* 2020. Reconstructing Tonian seawater $^{87}Sr/^{86}Sr$ using calcite microspar. *Geology*, **48**, 462–467, https://doi.org/10.1130/G46756.1